Early Disk-Galaxy Formation from JWST to the Milky Way
Proceedings IAU Symposium No. 377, 2024
F. Tabatabaei, B. Barbuy & Y.-S. Ting, eds.
doi:10.1017/S1743921323001072

Massive-Star Feedback at Low Metallicity

M. S. Oey[1], M. C. Jecmen[1], A. N. Sawant[1,2], A. E. Jaskot[3], A. Danehkar[4] L. J. Smith[5] and J. Melinder[6]

[1]University of Michigan, Department of Astronomy, Ann Arbor, MI, 48109, USA.
email: msoey@umich.edu

[2]Current address: EPFL, Institute of Mathematics, MA C2 647, Station 8, CH-1015 Lausanne, Switzerland

[3]Williams College, Department of Astronomy, Williamstown, MA 01267, USA

[4]Current address: Eureka Scientific, 2452 Delmer St., Suite 100, Oakland, CA 94602, USA

[5]Space Telescope Science Institute, 3700 San Martin Drive, Baltimore, MD 21218, USA

[6]Stockholm University, Department of Astronomy, Oscar Klein Centre, AlbaNova University Centre, SE-10691 Stockholm, Sweden

Abstract. Early cosmic epochs are characterized by low metallicity and high specific star-formation rates. These conditions are dominated by massive-star feedback that may be dramatically different than the traditional model dominated by hot, thermal superwinds driven by supernova explosions. Instead, metal-poor feedback from massive stars may be radiation-dominated, with weak mechanical feedback, possibly aiding the escape of Lyα and Lyman continuum radiation. I will describe our understanding that is emerging from observations of starburst galaxies in the local universe.

Keywords. massive stars — galactic winds — superbubbles — young massive clusters — core-collapse supernovae — starburst galaxies — emission-line galaxies — galaxy evolution — reionization

1. Mechanical Feedback at Low Metallicity

Mechanical feedback from the stellar winds and supernovae (SNe) of massive stars is a major driver of galaxy evolution. It is responsible for generating the hot, coronal-gas component of the interstellar medium (ISM), superbubbles, and superwinds from starbursts that are seen in X-ray observations of starburst galaxies. This hot gas carries the nucleosynthesis products from SNe and massive stars, thereby dispersing these metals and driving galactic chemical evolution. Mechanical feedback is also believed to promote the escape of Lyman continuum (LyC) radiation from starbursts by clearing out gas, thereby opening channels for LyC and Lyα photons (e.g., Heckman et al. 2011; Zastrow et al. 2013).

The classical scenario for mechanical feedback is based on an energy-driven model where massive-star winds and SNe shock-heat the surrounding gas, driving a cool, dense shell enclosing a low-density, adiabatic, hot interior (e.g., Weaver et al. 1977; Mac Low & McCray 1988); or similarly a hot, adiabatic, freely expanding superwind (Chevalier & Clegg 1985). However, this paradigm shifts dramatically at low metallicity, for several reasons. First, stellar winds are line-driven and therefore intrinsically weak at low metallicity. This is then compounded by the expectation that the most massive stars do not explode and instead collapse directly to black holes. The classical scenario at

© The Author(s), 2024. Published by Cambridge University Press on behalf of International Astronomical Union.

https://doi.org/10.1017/S1743921323001072 Published online by Cambridge University Press

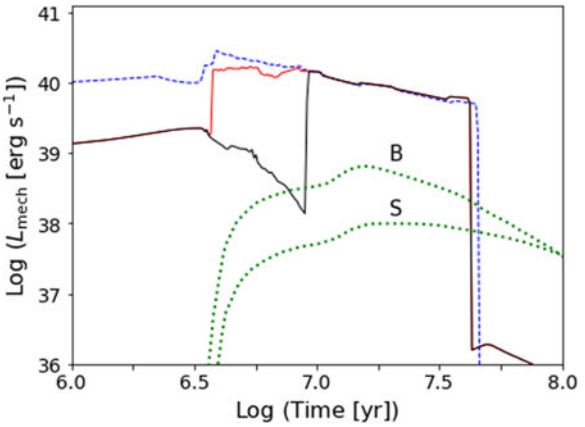

Figure 1. Total mechanical luminosity for stellar winds and SNe calculated from Starburst99 as a function of time for a 10^6 $M_\odot$ single stellar population. The dashed blue line shows the classical $Z_\odot = 0.014$ model with SNe starting at 3 Myr, based on evolutionary models for rotating stars by Ekström et al. (2012). The red solid line is the same but for subsolar metallicity from models by Georgy et al. (2013) at $Z = 0.002$. The black solid line is the same as the red line but for SN progenitors restricted to masses of $8 - 23$ $M_\odot$. The dotted green lines show estimates of HMXB feedback from Rappaport et al. (2005) with (B) and without (S) strong super-Eddington enhancement. (From Jecmen & Oey 2023, in preparation)

solar metallicity ($Z_\odot$) is that for a single stellar population with a Salpeter (1955) IMF, the combined stellar winds have roughly the same mechanical power L as the subsequent SNe, which are assumed to start at an age of 3 Myr, and thus $L(t)$ is approximately constant over massive-star lifetimes (~ 40 Myr). However, models suggest that SNe largely originate from stars $\lesssim 20$ $M_\odot$ at low metallicity (Heger *et al.* 2003; Zhang et al. 2008; O'Connor & Ott 2011; Sukhbold et al. 2016). This causes the onset of SNe to start around 10 Myr, rather than 3 Myr.

Figure 1 compares Starburst99 population synthesis models (Leitherer et al. 2014) for the classical scenario at $Z_\odot$ with their "subsolar" models. We also restrict SN progenitors in the subsolar models to stars with zero-age main sequence masses of $8 - 23$ $M_\odot$ instead of $8 - 120$ $M_\odot$ for $Z_\odot$. Figure 1 shows a factor of ~ 10 decrease in L at early times, which begins to drop precipitously once the most massive stars collapse into black holes after 3 Myr. There are minor effects that counteract this trend, for example, SNe are not necessarily completely eliminated at early times since stellar core explodability is stochastic (e.g., Sukhbold et al. 2016), and pair-instability SNe may also occur for the highest-mass progenitors (e.g., Heger *et al.* 2003). Additionally, Wolf-Rayet (WR) winds may be strong, even at low metallicity (e.g., Vink et al. 2011). But overall, low-Z mechanical feedback effectively only begins around 10 Myr, once the SNe for ~ 20 $M_\odot$ stars begin (Jecmen & Oey 2023, in preparation).

Justham & Schawinski (2012) suggest that feedback from high-mass X-ray binaries (HMXBs) and ultraluminous X-ray sources (ULXs) might fill this pre-SN gap in L. Figure 1 shows binary population synthesis models of the Eddington luminosity $L_{\rm Edd}$ from Rappaport et al. (2005) overplotted in the dotted green lines, for a population of accreting 10 $M_\odot$ black holes normalized to the Starburst99 models. Their models B and S are with and without strong ($10\times$) super-Eddington enhancement, respectively. The figure shows that ordinary HMXBs seem unlikely to significantly contribute mechanical feedback, although these models do not account for more massive black holes nor neutron stars. Individual ULXs also have $L_X \gtrsim 10^{39}$ erg s^{-1}, and they could stochastically

https://doi.org/10.1017/S1743921323001072 Published online by Cambridge University Press

contribute in some systems, but their general importance at these early times is unclear (Jecmen & Oey 2023, in preparation).

Intrinsically weak and delayed feedback causes large quantities of high-density gas to be retained near young, massive star clusters. This causes the delayed, energy-driven feedback to be further suppressed. The gas-rich environment is more prone to mass-loading of incipient hot winds, which can cause catastrophic cooling, preventing them from fully developing (e.g., Silich et al. 2004; Tenorio-Tagle et al. 2007; Wünsch et al. 2008). Additionally, the high-density environment causes pressure confinement of expanding superbubbles (e.g., Oey & García-Segura 2004; Smith et al. 2006; Silich et al. 2007). Both of these effects can also slow the development or expansion of fully adiabatic systems (Danehkar et al. 2021). The parameter space for where these different effects dominate is explored by Danehkar et al. (2021).

2. Observational Evidence for Weak Early Feedback

Observational evidence is building in support of this revised paradigm for weak mechanical feedback in metal-poor conditions. It provides a natural explanation for the "superbubble power problem" (e.g., Oey et al. 2009). Observations of OB superbubbles in the Magellanic Clouds are typically observed to be too small relative to their observed stellar populations (e.g., Oey 1996; Cooper et al. 2004; Smith & Wang 2004; Ramachandran et al. 2019). Some objects in the Milky Way also show this problem (Saken et al. 1992; Brown et al. 1995), suggesting that $Z_\odot$ stars may not all explode either, although other possible effects may be important (Oey et al. 2009). There are also examples of starburst systems that show no evidence of classical superwinds. NGC 5253-D1 is the best known example (Turner et al. 2003), where a $\sim 10^5\ M_\odot$ super star cluster (SSC) is embedded within a dense knot of gas only 3 pc in radius, with no immediate evidence of an associated shell or chimney.

Mrk 71 in NGC 2366 is the nearest starburst system showing suppressed superwinds. This metal-poor ($Z \sim 0.1 Z_\odot$) object is an analog of the Green Pea galaxies, which are a local class of LyC emitters (e.g., Izotov et al. 2018; Flury et al. 2022). Mrk 71 is only 3.4 Mpc distant, and shows a clear view of the dominant star-forming complex (Figure 2a). The Green Pea properties are driven by the $\sim 10^5\ M_\odot$ SSC in Knot A (Micheva et al. 2017). The gas kinematics around this object are fully consistent with only momentum-conserving feedback instead of energy-driven feedback (Komarova et al. 2021; Oey et al. 2017).

The most extreme Green Pea galaxies also show evidence of suppressed superwinds. Jaskot et al. (2017) used HST/COS observations of a sample of Green Peas to compare superwind velocities, probed by Si III and Si IV absorption, with neutral gas content in the line of sight, as indicated by the equivalent width (EW) of low-ionization species, mostly Si II. Figure 3 shows the expected dominant correlation between strong, blueshifted superwinds, and low EW in the low-ionization species. However, a prominent group of objects with the most extreme [O III]/[O II] ionization parameters shows the opposite effect: the objects with the lowest Si II EW also show the weakest hot superwind velocities. This suggests that the most extreme Green Pea objects may host the youngest populations and lowest metallicities, and may be observed well before mechanical feedback develops. This also explains their extreme ionization parameters, which are a signature of radiation-dominated conditions.

Other higher-ionization nebular emission lines also point to possible radiation-dominated conditions, while some may also indicate strong radiative cooling of shock-heated gas from weakened outflows. In particular, nebular He II 1640, He II 4686, and C IV 1550 are species often seen in Green Peas and similar extreme, metal-poor starbursts across the universe, at low (e.g., Berg et al. 2018), moderate (e.g. Amorín et al.

https://doi.org/10.1017/S1743921323001072 Published online by Cambridge University Press

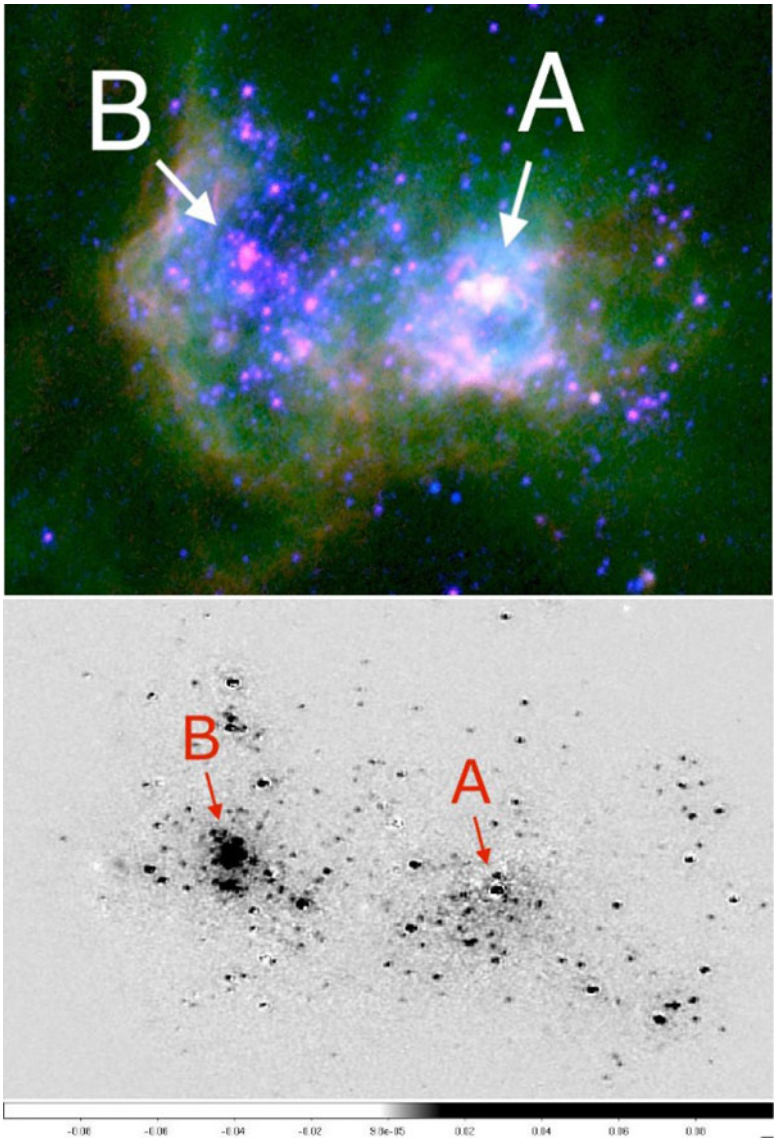

Figure 2. Panel *a* (top) shows Hubble Space Telescope (HST) WFC3 imaging of Mrk71 complex in NGC 2366. Red, green, and blue show F373N ([O II] 3727), F502N ([O III] 5007), and F438W, respectively. The nebular line imaging is continuum subtracted data from James (2016). The SSCs Knots A and B are indicated, and they are separated by 85 pc. North is up, and east to the left. Panel *b* (bottom) shows HST/ACS-SBC imaging in F150LP with F165LP subtracted, revealing C IV 1550 emission. (From Oey et al. 2023, in preparation.)

2017), and high (Stark et al. 2015) redshifts. While these species may be indicative of unusually hard photoionizing sources, they also may be due to catastrophic cooling of outflows (Gray et al. 2019; Danehkar et al. 2021, 2022). To more clearly evaluate the origin of nebular C IV 1550 emission, we have obtained the first-ever, resolved nebular imaging in this doublet. The observations were done with the ACS/SBC camera aboard HST in Cycle 28 (Program 16261, PI: Oey), using the long-pass filters F150LP and F165LP. The difference of these filters yields an effective bandpass with FWHM ~ 160 Å that captures C IV 1550. Our preliminary results are shown in Figure 2b. Diffuse, extended

https://doi.org/10.1017/S1743921323001072 Published online by Cambridge University Press

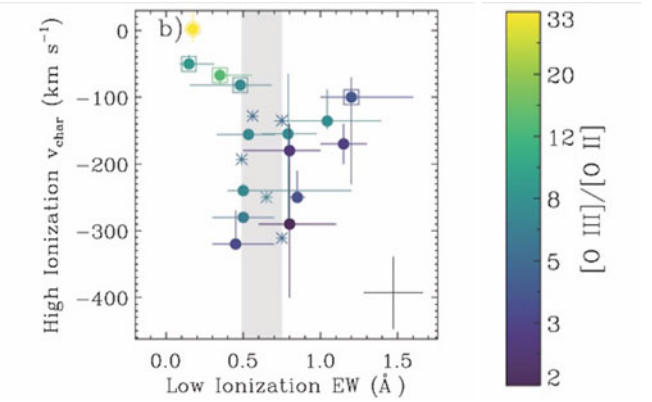

Figure 3. Blueshifted superwind velocities measured from Si III 1206 and Si IV 1400 vs median EW of a series of O I, Si II, and C II absorption lines in HST/COS data for a sample of Green Peas. The [O III] 5007 / [O II] 3727 ratio is shown by the color scale. (From Jaskot et al. 2017)

C IV emission is seen in a $\sim$20-pc radius around the Knot A SSC. Modeling is underway to evaluate whether this nebular C IV is due to catastrophic cooling or photoionization.

Numerous point sources are also apparent in Figure 2b. These are likely mostly O stars with C IV wind emission. Knot A shows C IV stellar wind emission that may be due to very massive stars (VMS) $> 100\ M_\odot$, as suggested by the presence of He II 1640 wind emission seen in HST/STIS spectra (Smith et al. 2023, in preparation). There are also several luminous WR stars present, especially in Knot B, which is known to contain at least 3 WR stars (Drissen et al. 2000). As seen in Figure 2a, Knot B is driving a conventional superbubble and chimney system (Micheva et al. 2017). Ordinarily, the presence of WR stars would suggest an age of $\sim$5 Myr (e.g., Drissen et al. 2000). However, the presence of the superbubble and chimney, as well as diffuse X-ray emission (Thuan et al. 2014), indicate that at least several SNe have occurred. Given our new paradigm for metal-poor systems in which the onset of SNe occurs later than classically expected, the age of the Knot B region seems likely to be closer to 10 – 12 Myr. This would in turn require that the WR stars are much older than 5 Myr. One possibility is that they could be rapidly rotating mass-gainers that evolved to hotter temperatures as a result of chemically homogeneous evolution. We are carrying out more detailed study of the stellar population with HST/STIS observations to evaluate the evolutionary state of the cluster and these WR stars.

3. A Scenario for Feedback at Low Metallicity

If, at low metallicity, energy-driven mechanical feedback effectively does not start until $\sim$10 Myr, then this has profound consequences for the nature of massive-star feedback. In the first instance, superbubbles driven by OB associations at low metallicity are expected to be smaller, and developing later, relative to their high-metallicity counterparts. The total amount of hot gas generated per specific star-formation rate is somewhat less, which may modify the phase balance of the ISM and circumgalactic medium. This, in turn, affects the dispersal of metals, causing somewhat slower galactic chemical evolution (Semenov et al. 2021). The revised mass range for SN progenitors also generates different nucleosynthesis products. The cumulative total differences in mechanical energy and metal injection between the classical, $Z_\odot$ scenario and the subsolar, weak feedback model (black line in Figure 1) are less than a factor of two. However, the the delay at early times occurs during the lifetimes of the most luminous, LyC-emitting stars, fundamentally altering the nature of massive-star feedback, as follows.

https://doi.org/10.1017/S1743921323001072 Published online by Cambridge University Press

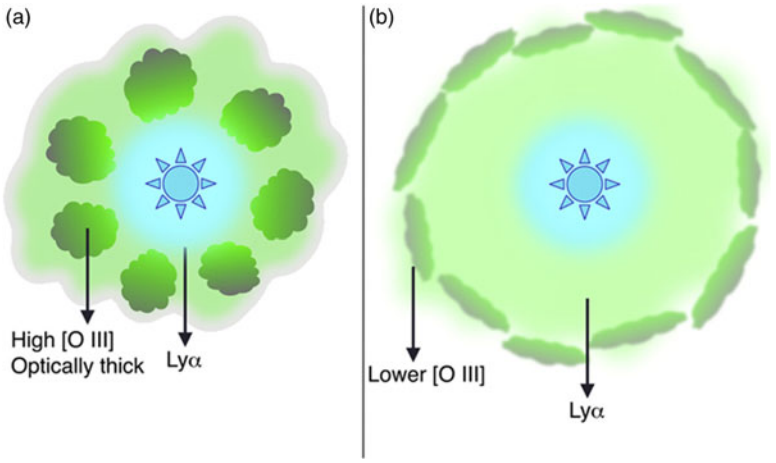

Figure 4. Comparison of models for low- (panel *a*, left) and high-metallicity (panel *b*, right) massive-star feedback. The low-Z model has weak mechanical feedback, and dense, clumped gas remains close to the SSC. In this radiation-dominated environment, the optically thick clumps generate high surface brightness and high ionization parameter, while the low-density gaps allow escape of LyC and Lyα photons. In contrast, large quantities of gas are piled up far from the SSC at high Z, promoting optically thick conditions and lower ionization parameters. (From Jaskot et al. 2019)

The retention of dense gas and molecular clouds likely leads to clumping on both large and small scales. Outflows from radiation pressure and stellar winds are still significant (e.g., Dopita et al. 2002; Krumholz & Thompson 2012), and would therefore cause dynamical instabilities like Rayleigh-Taylor, Vishniac (1983), and Giuliani (1979) instabilities. Additionally, dense clumps can also become thermally unstable, promoting continued star formation. Some have therefore suggested weak mechanical feedback to be linked to multiple stellar populations in globular clusters (e.g., Krause et al. 2012; Silich & Tenorio-Tagle 2018). Indeed, the immediate environment of Knot A in Mrk 71 shows the presence of 10^5 $M_\odot$ molecular clouds within a few pc of the SSC (Oey et al. 2017).

As noted above, we expect SN feedback to only start at an age where stars $\lesssim 20$ $M_\odot$ collapse. But the higher-mass stars are those that strongly dominate the production of LyC radiation, and therefore, in the absence of mechanical feedback, the early period < 10 Myr is strongly dominated by radiation feedback (e.g., Freyer et al. 2003; Krumholz & Matzner 2009). Together with strong clumping of the dense gas near the parent SSC, low-density windows may form that allow LyC radiation to escape (Figure 4; Jaskot et al. 2019). This scenario naturally explains the picket-fence morphology that is frequently inferred in extreme starbursts (e.g., Heckman et al. 2011; Rivera-Thorsen et al. 2015). It also circumvents the problem with classical mechanical feedback that superwinds can pile up gas into large, optically thick shells that impede LyC escape (e.g., Dove et al. 2000), as illustrated in Figure 4. The presence of a large-scale (300 pc), 3500 km s^{-1}, LyC-driven superwind from Knot A in Mrk 71 appears to support this scenario, since continued acceleration of such a wind requires low LyC and/or Lyα optical depth at large distances (Komarova et al. 2021), while large quantities of dense gas and molecular clouds are also seen at close quarters to the SSC.

4. Summary

In summary, in metal-poor environments, stellar winds are weak and SNe start later than at solar metallicity. This implies that classical mechanical feedback in the form of

https://doi.org/10.1017/S1743921323001072 Published online by Cambridge University Press

energy-driven, adiabatic flows, is effectively delayed until ages on the order of 10 Myr. The effect is compounded by the retained dense gas further inhibiting the development of mechanical feedback by promoting catastrophic cooling, pressure confinement, and longer wind launching times.

There is growing observational evidence for this scenario. Superbubbles are known to be smaller than expected for observed parent stellar populations, and there are observed examples of nearby starbursts and extreme Green Pea galaxies that lack any evidence of energy-driven superwinds.

This implies a shift in the paradigm for massive star feedback at low metallicity, such that it is dominated by radiation feedback rather than mechanical feedback at ages $\lesssim 10$ Myr. Dense gas is retained in the environment at early times, promoting clumping by dynamical and gravitational instabilities. This leads to enhanced and continued star formation, as well as the possible escape of LyC and Lyα radiation through gaps between the clumps. Earlier presentations at this conference of new JWST data demonstrate that starburst galaxies at redshifts of $z = 5$ to 10 are indeed high-redshift analogs of Green Peas (e.g., Maiolino 2023). Therefore the revised paradigm for metal-poor feedback is likely important in this regime.

Acknowledgements

This work was supported by NASA grant HST-GO-16261 and the University of Michigan. M.S.O. is also grateful to the conference organizers and the IAU for a registration fee waiver. We also thank Sergiy Silich, Claus Leitherer, Edmund Hodges-Kluck, and others for discussions over many years.

References

Amorín, R., et al. 2017, Nature Astronomy, 1, 0057
Berg, D. A., Erb, D. K., Auger, M. W., Pettini, M., & Brammer, G. B. 2018, ApJ, 859, 164
Brown, A. G. A., Hartmann, D., & Burton, W. B. 1995, A&A, 300, 903
Chevalier, R. A., & Clegg, A. W. 1985, Nature, 317, 44
Cooper, R. L., Guerrero, M. A., Chu, Y.-H., Chen, C. H. R., & Dunne, B. C. 2004, ApJ, 605, 751
Danehkar, A., Oey, M. S., & Gray, W. J. 2021, ApJ, 921, 91
—. 2022, ApJ, 937, 68
Dopita, M. A., Groves, B. A., Sutherland, R. S., Binette, L., & Cecil, G. 2002, ApJ, 572, 753
Dove, J. B., Shull, J. M., & Ferrara, A. 2000, ApJ, 531, 846
Drissen, L., Roy, J.-L., Robert, C., & Devost, D. 2000, AJ, 119, 688
Ekström, S., et al. 2012, A&A, 537, A146
Flury, S. R., et al. 2022, ApJS, 260, 1
Freyer, T., Hensler, G., & Yorke, H. W. 2003, ApJ, 594, 888
Georgy, C., et al. 2013, A&A, 558, A103
Giuliani, J. L., J. 1979, ApJ, 233, 280
Gray, W. J., Oey, M. S., Silich, S., & Scannapieco, E. 2019, ApJ, 887, 161
Heckman, T. M., et al. 2011, ApJ, 730, 5
Heger, A., Fryer, C. L., Woosley, S. E., Langer, N., & Hartmann, D. H. 2003, ApJ, 591, 288
Izotov, Y. I., Worseck, G., Schaerer, D., Guseva, N. G., Thuan, T. X., Fricke, Verhamme, A., & Orlitová, I. 2018, MNRAS, 478, 4851
James, B. L., Auger, M., Aloisi, A., Calzetti, D., & Kewley, L. 2016, ApJ, 816, 40
Jaskot, A. E., Dowd, T., Oey, M. S., Scarlata, C., & McKinney, J. 2019, ApJ, 885, 96
Jaskot, A. E., Oey, M. S., Scarlata, C., & Dowd, T. 2017, ApJL, 851, L9
Justham, S., & Schawinski, K. 2012, MNRAS, 423, 1641
Komarova, L., Oey, M. S., Krumholz, M. R., Silich, S., Kumari, N., & James, B. L. 2021, ApJL, 920, L46

https://doi.org/10.1017/S1743921323001072 Published online by Cambridge University Press

Krause, M., Charbonnel, C., Decressin, T., Meynet, G., Prantzos, N., & Diehl, R. 2012, A&A, 546, L5
Krumholz, M. R., & Matzner, C. D. 2009, ApJ, 703, 1352
Krumholz, M. R., & Thompson, T. A. 2012, ApJ, 760, 155
Leitherer, C., Ekström, S., Meynet, G., Schaerer, D., Agienko, K. B., & Levesque, E. M. 2014, ApJS, 212, 14
Mac Low, M.-M., & McCray, R. 1988, ApJ, 324, 776
Maiolino, R. 2023, these proceedings
Micheva, G., Oey, M. S., Jaskot, A. E., & James, B. L. 2017, ApJ, 845, 165
O'Connor, E., & Ott, C. D. 2011, ApJ, 730, 70
Oey, M. S. 1996, ApJ, 467, 666
Oey, M. S., & García-Segura, G. 2004, ApJ, 613, 302
Oey, M. S., Herrera, C. N., Silich, S., Reiter, M., James, B. L., Jaskot, A. E., & Micheva, G. 2017, ApJL, 849, L1
Oey, M. S., Smith, R. K., Snowden, S. L., & Kuntz, K. D. 2009, in AIP Conference Proceedings, Vol. 1156 (AIP), 295–304
Ramachandran, V., et al. 2019, A&A, 625, A104
Rappaport, S. A., Podsiadlowski, P., & Pfahl, E. 2005, MNRAS, 356, 401
Rivera-Thorsen, T. E., et al. 2015, ApJ, 805, 14
Saken, J. M., Fesen, R. A., & Shull, J. M. 1992, ApJS, 81, 715
Salpeter, E. E. 1955, ApJ, 121, 161
Semenov, V. A., Kravtsov, A. V., & Gnedin, N. Y. 2021, ApJ, 918, 13
Silich, S., & Tenorio-Tagle, G. 2018, MNRAS, 478, 5112
Silich, S., Tenorio-Tagle, G., & Muñoz-Tuñón, C. 2007, ApJ, 669, 952
Silich, S., Tenorio-Tagle, G., & Rodríguez-González, A. 2004, ApJ, 610, 226
Smith, D. A., & Wang, Q. D. 2004, ApJ, 611, 881
Smith, L. J., Westmoquette, M. S., Gallagher, J. S., O'Connell, R. W., Rosario, D. J., & de Grijs, R. 2006, MNRAS, 370, 513
Smith, L. J., Oey, M. S., Hernandez, S. et al. 2023, arXiv231003413S
Stark, D. P., et al. 2015, MNRAS, 454, 1393
Sukhbold, T., Ertl, T., Woosley, S. E., Brown, J. M., & Janka, H. T. 2016, ApJ, 821, 38
Tenorio-Tagle, G., Wünsch, R., Silich, S., & Palouš, J. 2007, ApJ, 658, 1196
Thuan, T. X., Bauer, F. E., & Izotov, Y. I. 2014, MNRAS, 441, 1841
Turner, J. L., Beck, S. C., Crosthwaite, L. P., Larkin, J. E., McLean, I. S., & Meier, D. S. 2003, Nature, 423, 621
Vink, J. S., Muijres, L. E., Anthonisse, B., de Koter, A., Gräfener, G., & Langer, N. 2011, A&A, 531, A132
Vishniac, E. T. 1983, ApJ, 274, 152
Weaver, R., McCray, R., Castor, J., Shapiro, P., & Moore, R. 1977, ApJ, 218, 377
Wünsch, R., Tenorio-Tagle, G., Palouš, J., & Silich, S. 2008, ApJ, 683, 683
Zastrow, J., Oey, M. S., Veilleux, S., & McDonald, M. 2013, ApJ, 779, 76
Zhang, W., Woosley, S. E., & Heger, A. 2008, ApJ, 679, 639

https://doi.org/10.1017/S1743921323001072 Published online by Cambridge University Press